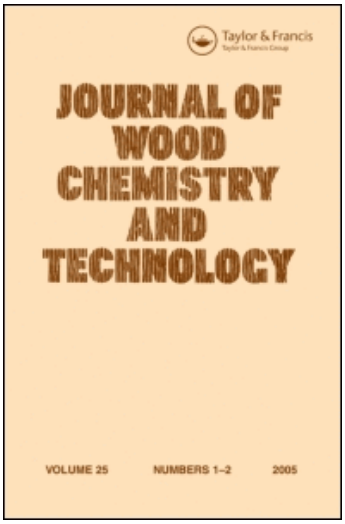

Journal of Wood Chemistry and Technology
Publication details, including instructions for authors and subscription information:
http://www.informaworld.com/smpp/title~content=t713597282

Reactivity of the Carbonate Radical Anion Towards Carbohydrate and Lignin Model Compounds

David Stenman[a]; Magnus Carlsson[a]; Mats Jonsson[a]; Torbjörn Reitberger[a]
[a] Department of Chemistry-Nuclear Chemistry, Royal Institute of Technology, Stockholm, Sweden

Online publication date: 18 March 2003

To cite this Article Stenman, David , Carlsson, Magnus , Jonsson, Mats and Reitberger, Torbjörn(2003) 'Reactivity of the Carbonate Radical Anion Towards Carbohydrate and Lignin Model Compounds', Journal of Wood Chemistry and Technology, 23: 1, 47 — 69
To link to this Article: DOI: 10.1081/WCT-120018615
URL: http://dx.doi.org/10.1081/WCT-120018615

MARCEL DEKKER, INC. • 270 MADISON AVENUE • NEW YORK, NY 10016

JOURNAL OF WOOD CHEMISTRY AND TECHNOLOGY
Vol. 23, No. 1, pp. 47–69, 2003

Reactivity of the Carbonate Radical Anion Towards Carbohydrate and Lignin Model Compounds

David Stenman, Magnus Carlsson, Mats Jonsson, and Torbjörn Reitberger*

Department of Chemistry-Nuclear Chemistry, Royal Institute of Technology, Stockholm, Sweden

ABSTRACT

The kinetic selectivity for the reaction of the carbonate radical anion towards lignin and carbohydrate model compounds was determined by pulse radiolysis in the pH-span 8–13. For the cellulose model compound methyl-β-D-glucopyranoside a pK_A-value of 14.4 was estimated.

Key Words: Carbonate radical anion; Selectivity; Pulp; Bleaching.

*Correspondence: Torbjörn Reitberger, Department of Chemistry-Nuclear Chemistry, Royal Institute of Technology, Teknikringen 56, SE-100 44 Stockholm, Sweden; Fax: 4687908772; E-mail: torbreit@nuchem.kth.se.

DOI: 10.1081/WCT-120018615 0277-3813 (Print); 1532-2319 (Online)

INTRODUCTION

Oxidative delignification of wood pulp using oxygen, ozone, or hydrogen peroxide inevitably leads to the formation of hydroxyl radicals, $HO^{\bullet}$, and superoxide, $O_2^{\bullet -}$. The presence of these radicals increases the extent of delignification but it also limits the selectivity of the process due to autoxidation cycles in the fibres.[1]

To deepen our understanding of how radicals react with both lignin and cellulose in pulp, it is of interest to study the effect of other relevant radicals towards these structures. One such radical is the carbonate radical anion, which is a strong oxidant with a one-electron reduction potential of 1.59 V vs. NHE at $pH > 10.3$.[2] Like the hydroxyl radical, the carbonate radical can attack organic substances via electron-transfer or H-atom abstraction mechanisms. With certain radicals the carbonate radical anion may also react by an $O^{\bullet -}$-transfer.[3]

The carbonate radical anion is conveniently generated by photolysis or radiolysis of carbonate solutions or by reacting peroxynitrite with carbon dioxide, *vide infra*. It can be directly detected using ESR,[4,5] as well as by optical spectroscopy. The carbonate radical anion exhibits a strong absorption peak around 600 nm,[6] a wavelength usually well separated from that of other species. For kinetic studies, a spectroscopic system is usually combined with flash photolysis[7–12] or pulse radiolysis.[2,3,6,13–19]

It is now well established that the carbonate radical remains a mono-anion over the whole pH-range,[20] i.e., the radical per se is pH-invariant. These properties suggest that the carbonate radical anion is a suitable oxidative probe for studying the effects of pH on the reactivity of different lignin and carbohydrate structures, using suitable model compounds. This is the principal aim of this study. There is also another objective of a more practical nature. Improved selectivity and yield have been observed in oxygen bleaching when carbonate has been used as the base.[21] Therefore, we have determined the kinetic selectivity of the carbonate radical anion towards lignin and carbohydrate model compounds in the pH-range 8–13.

Under oxygen bleaching conditions using carbonate as base a more rapid oxidation of a phenolic model compound was observed.[22] This indicates that carbonate may also have other interesting effects in oxygen bleaching.

In recent years, considerable interest has been focused on the carbonate radical since evidence has accumulated that it occurs in the human body due to a reaction between carbon dioxide and peroxynitrite.[23]

The latter is formed when nitrogen monoxide reacts with superoxide. Thus, oxidative damage caused by superoxide may be mediated by the carbonate radical and its possible medical/biochemical importance has inspired several studies.[24–26] Due to its reactivity, it has also been suggested that the carbonate radical may be a suitable oxidant of water pollutants.[7] Some of these previous studies have been done using pulse radiolysis or flash photolysis on different aromatic substances of relevance to this study. Work on glucose by flash photolysis has also been reported.[8]

EXPERIMENTAL

1. Generation of the Carbonate Radical Anion

Radiolysis of water will produce hydroxyl radicals, solvated electrons, and hydrogen atoms, as well as minor amounts of hydrogen peroxide and H_2.[27] The radicals initially formed can, by different methods, be interconverted or directed towards the formation of new radical species. A convenient and widely used method of improving the hydroxyl radical yield during radiolysis of water solutions is by saturating such solutions with N_2O, which leads to capture of solvated electrons and subsequent OH-radical formation.[28] In such a system, the hydroxyl radical yield approaches 95% of the total radical yield, with hydrogen atoms constituting the remaining yield.

The hydroxyl radicals thus produced can react with carbonate or bicarbonate in solution to produce the carbonate radical anion.[28] The rate of this reaction is pH-controlled, as the carbonate and bicarbonate ions show different reactivities towards the hydroxyl radical[28]:

$$CO_3^{2-} + HO^{\bullet} \xrightarrow{k_1} CO_3^{\bullet -} + OH^- \qquad k_1 = 3.9 \times 10^8\ M^{-1}\,s^{-1} \tag{1}$$

$$HCO_3^- + HO^{\bullet} \xrightarrow{k_2} CO_3^{\bullet -} + H_2O \qquad k_2 = 8.5 \times 10^6\ M^{-1}\,s^{-1} \tag{2}$$

In these experiments, the hydroxyl radicals produced will also react with the substrate, S, as described by:

$$S + HO^{\bullet} \xrightarrow{k_3} \text{products} \tag{3}$$

For both lignin and cellulose structures this reaction is diffusion-controlled, i.e., the reaction rate constant, k_3, is in the range of 10^9–$10^{10}\ M^{-1}\,s^{-1}$.[29]

Table 1. Compositions of the carbonate buffer solutions.

pH	$NaHCO_3$ (M)	Na_2CO_3 (M)	NaOH
8.3	Saturated	0	0
9.3	0.85	0.15	0
10.3	0.5	0.5	0
11	0.15	0.85	0
12	0	1	0
13	0	1	0.1

With an excess of carbonate over the substrate, most of the initial hydroxyl radicals formed can be directed towards the formation of carbonate radical anions. The concentration ratio needed for at least 90% carbonate radical anion production can be calculated from:

$$\frac{k_3[\mathrm{S}]}{k_1[\mathrm{CO}_3^{2-}] + k_2[\mathrm{HCO}_3^-]} < 0.1 \tag{4}$$

For practical reasons the carbonate concentration should not exceed 1 M. Thus, according to Eq. (4), the substrate concentration must be limited to the mM-range (depending on pH).

The pH was adjusted by varying the ratio of $[CO_3^{2-}]$ to $[HCO_3^-]$. For pH > 12, NaOH was added. The composition of carbonate buffers is shown in Table 1. All samples were diluted using stock solutions of carbonate to minimise dilution errors.

2. Kinetic Measurements

In this study, we have applied pulse radiolysis to obtain spectral and kinetic data by observing the formation and decay of short-lived radical species. The radiation source was a 3 MeV linear accelerator (Linac) delivering a dose of approx. 10 Gy/pulse. The radical concentration initially produced was in the micromolar range (1–5 μM). A 1 cm thermostatable flow cell (Helma 164.000-QS) was employed. For spectroscopic measurements, a computerised optical detection system was used, as described elsewhere.[30] Under ideal conditions, the system has a time resolution of approx. 10 ns. In some experiments, the light source was a 6 mW diode laser emitting at 635 nm, a wavelength close to the absorption peak of $CO_3^{\bullet-}$ at 600 nm.[6]

For the kinetic measurements, the decay of the carbonate radical anions formed after irradiation of the sample was measured at ambient conditions, i.e., 25°C, unless otherwise stated. The decay was a result of the second order reaction between substrate and radicals described by:

$$\frac{d[CO_3^{\bullet -}]}{dt} = -k[S][CO_3^{\bullet -}] \tag{5}$$

As the amount of substrate present in the system was much larger than the amount of radicals formed from the pulse, the change in substrate concentration can be regarded as insignificant, which implies that Eq. (5) can be rewritten as a *pseudo*-first order decay of the carbonate radical anion:

$$\frac{d[CO_3^{\bullet -}]}{dt} = -k^*[CO_3^{\bullet -}] \tag{6}$$

$$k^* = k[S]$$

where variations in [S] will be insignificant.

Integration of Eq. (6) leads to:

$$[CO_3^{\bullet -}] = [CO_3^{\bullet -}]_0 e^{-k^* t}$$
$$\text{i.e.,} \quad A = A_0 e^{-k^* t} \tag{7}$$

where A is the measured absorbance at 600 nm. The logarithm of Eq. (7) is a linear function of absorbance over time, the slope of which is the *pseudo*-first order rate-constant.

By measuring the *pseudo*-first order rate constant at various substrate concentrations, the second order rate coefficient, k, in Eq. (5) can be obtained. To minimise radical losses in non-desirable termination reactions, the substrate concentration must be high enough to promote a fast substrate-radical reaction. By combining this restriction with that described by Eq. (4), we determined a range of substrate concentrations over which *pseudo*-first order kinetics could be measured. All calculations and numerical treatments of data were performed using Matlab® and Excel® software.

3. Radical Spectra

Radical spectra were obtained from measurements at different wavelengths of the optical absorbance observed immediately after the electron pulse. The dose per pulse was calibrated against the KSCN-dosimeter. An extinction coefficient of 7900 $M^{-1} cm^{-1}$ at 500 nm[27] was

Table 2. Compositions of the solutions used for spectral measurements.

Measurement	Composition
$CO_3^{\bullet-}$ with 1,2,4-tri-methoxybenzene	1 mM 1,2,4-tri-methoxybenzene, 1 M Na_2CO_3, N_2O saturated
$N_3^{\bullet}$ with 1,2,4-tri-methoxybenzene	1 mM 1,2,4-tri-methoxybenzene, 10 mM NaN_3, 0.01 M NaOH, N_2O saturated
$HO^{\bullet}$ with 1,2,4-tri-methoxybenzene	1 mM 1,2,4-tri-methoxybenzene, N_2O saturated
Dosimetry	10 mM KSCN, N_2O saturated

used for the $(SCN)_2^{\bullet-}$ radical. Spectra were obtained from solutions described in Table 2.

4. Materials

All chemicals used were of the purest grade available from commercial sources (Merck, Aldrich, Acros Organics). The water used was purified in a Millipore Milli-Q filter. In the pulse radiolysis experiments, all the solutions were N_2O-saturated in order to increase the $HO^{\bullet}$ yield by removal of solvated electrons, as mentioned above. All measurements were performed on fresh solutions.

RESULTS

For each substance, kinetic measurements were performed, and *pseudo*-first order reaction rate constants were obtained as functions of substrate concentration and pH. The measurements were evaluated according to Eq. (7). When the *pseudo*-first order rate constants were plotted against the substrate concentrations, a straight line was obtained. The slope of the linear plot gives the rate constant of the second order reaction, as described by Eq. (5). A typical plot is shown in Fig. 1.

The measured second order rate constants are summarized for all substituted benzenes/lignin models in Table 3 and for the carbohydrates in Table 4.

Initial spectra obtained after irradiation of the solutions described in Table 2 are shown in Fig. 2.

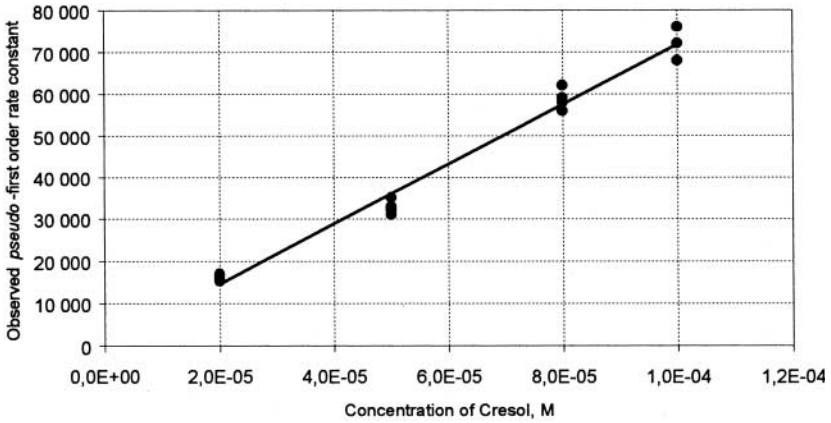

Figure 1. *Pseudo*-first order rate constants for the reaction of $CO_3^{\bullet-}$ with cresol at pH 10 vs. the cresol concentration.

Experiments to determine the activation energies over the temperature range 5–75°C for the reaction of $CO_3^{\bullet-}$ with the carbohydrate model compounds gave E_A-values of ~10 kJ/mol. No pH-dependence of E_A could be seen.

DISCUSSION

1. Aromatic/Lignin Structures

The reaction of the carbonate radical anion ($CO_3^{\bullet-}$) with 1,2,4-trimethoxybenzene (TMB) results in a transient species with spectral properties virtually identical to those of the azidyl radical ($N_3^{\bullet}$) and distinctly different from those given by the hydroxyl radical (Fig. 2). The azidyl radical has been shown to oxidise TMB quantitatively to give the corresponding radical cation.[31] Hence, we can conclude that the reaction of $CO_3^{\bullet-}$with TMB must proceed via electron transfer leading to the formation of a long-lived radical cation. It was noted that the spectrum after the OH-radical reaction showed some absorption above 380 nm with peaks at 420 and 470 nm. The peak at 470 nm coincided with that of the aromatic radical cation. After subtraction of the spectrum of the aromatic radical cation from that of the OH-radical reaction, the peak at 420 nm was enhanced, as shown in Fig. 3.

The absorption at 420 nm can be explained by the formation of phenoxyl radicals.[18,32] The reaction of the hydroxyl radical with TMB thus yields the hydroxyl radical adduct, as well as phenoxyl radicals and radical cations according to the following reactions:

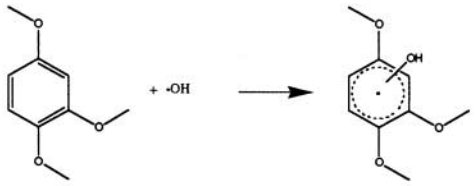

(1)

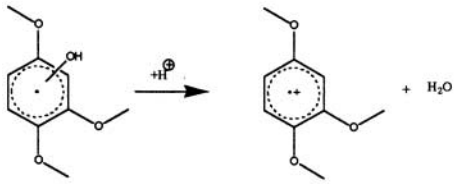

(2)

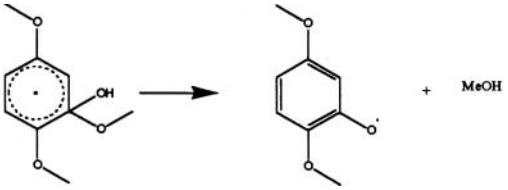

(3)

The radical cations formed, e.g., when $CO_3^{\bullet -}$ abstracts an electron from an aromatic, will undergo further reactions. It has been shown that aromatic radical cations can undergo β-bond cleavage in the side-chain[33] and can also react with H_2O/OH^- forming the hydroxyl radical adduct.[31,34] Such adducts may react further according to Reactions 2 or 3. One electron oxidation of phenols will directly form the corresponding phenoxyl radicals.

For one-electron transfer reactions, the free energy of reaction, ΔG°, and consequently the equilibrium constant, K (Eq. (8)), depends on the difference in redox potentials, ΔE°, between the two reacting substances (Eq. (9)):

$$\Delta G^0 = RT \ln K \tag{8}$$

$$\Delta G^0 = nF\Delta F^0 \tag{9}$$

In many cases, it has been shown that, when $\log k$ of a reaction is plotted vs. the corresponding $\log K$, a linear correlation is evident in similar reaction systems. Such linear free energy relationships, LFER,

Table 3. Rate constants for the reaction of the carbonate radical anion with lignin model compounds/substituted benzenes.

Substance	pH	Rate constant ($M^{-1} s^{-1}$)
4-Methylphenol	8.3	1.5×10^8
	10.3	7.1×10^8
	11	1.1×10^9
	12.1	1.2×10^9
o-Methoxy-phenoxyacetic acid	8	7.0×10^6
	12	7.3×10^6
2-Methoxy-4-methylphenol	8.3	1.7×10^8
	11	1.5×10^9
	12	6.0×10^8
Syringic acid	12	1.3×10^9
4-Methoxyphenol	12	1.1×10^9
3-Methoxyphenol	12	5.1×10^8
3,5-di-Methoxyphenol	12	5.9×10^8
3,4-di-Methoxy-acetophenone	12	5.6×10^8
Vanillin	8.3	1.0×10^8
	10.3	1.1×10^9
	11	1.1×10^9
	13	1.6×10^9
1,1′-Methoxy-5,5′-bi-phenol	12	5.7×10^8
2,4,6-tri-Methylphenol	10.3	5.2×10^8
	12	1.3×10^9
	13	2.7×10^9
6-Methoxy-4-*tert*-butylphenol	12	1.0×10^9
4,6-di-Chlororesorcinol	12	1.0×10^9
3,4-di-Methoxybenzoic acid	12	4.0×10^6
2,6-di-Methoxyphenol	12	1.4×10^9
3,4-di-Methoxy-phenylacetic acid	12	6.9×10^7

show that, as the reaction becomes more thermodynamically favorable, its reaction rate constant increases. For one electron transfer reactions, showing a LFER, $\log k$ should be proportional to the oxidation/reduction potentials of the substances involved.

The one-electron oxidation potentials of a number of substituted benzenes in aqueous solution have been previously determined by pulse radiolysis.[32,35,36] Furthermore, a relationship connecting the substituent pattern of substituted benzenes with their one-electron oxidation potentials has been previously reported.[37,38] This relationship can be

Table 4. Rate constants for the reaction of the carbonate radical anion with carbohydrate model compounds.

Substance	pH	Rate constant ($M^{-1} s^{-1}$)
Glucose	9.3	4.2×10^5
	10.3	1.06×10^5
	11	3.21×10^5
	12.1	2.26×10^6
	13	1.00×10^7
Methyl-beta-D-glucopyranoside	10.3	5.28×10^4
	11	3.88×10^4
	12.1	1.6×10^5
	13	7.47×10^5
Cellobiose	10.3	1.65×10^5
	11	3.07×10^5
	12.1	4.79×10^6
	13	1.08×10^7
Sucrose	8.3	2.37×10^4
	9.3	1.0×10^5
	10.3	2.4×10^4
	13	1.9×10^6

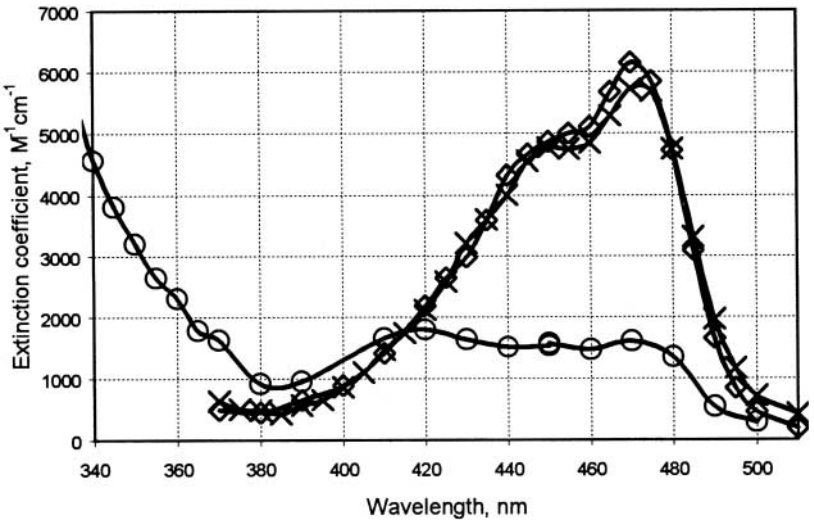

Figure 2. Initial spectra after reaction of the carbonate (X), azidyl (◇) and OH-radicals (○), respectively, with 1,2,4-tri-methoxybenzene.

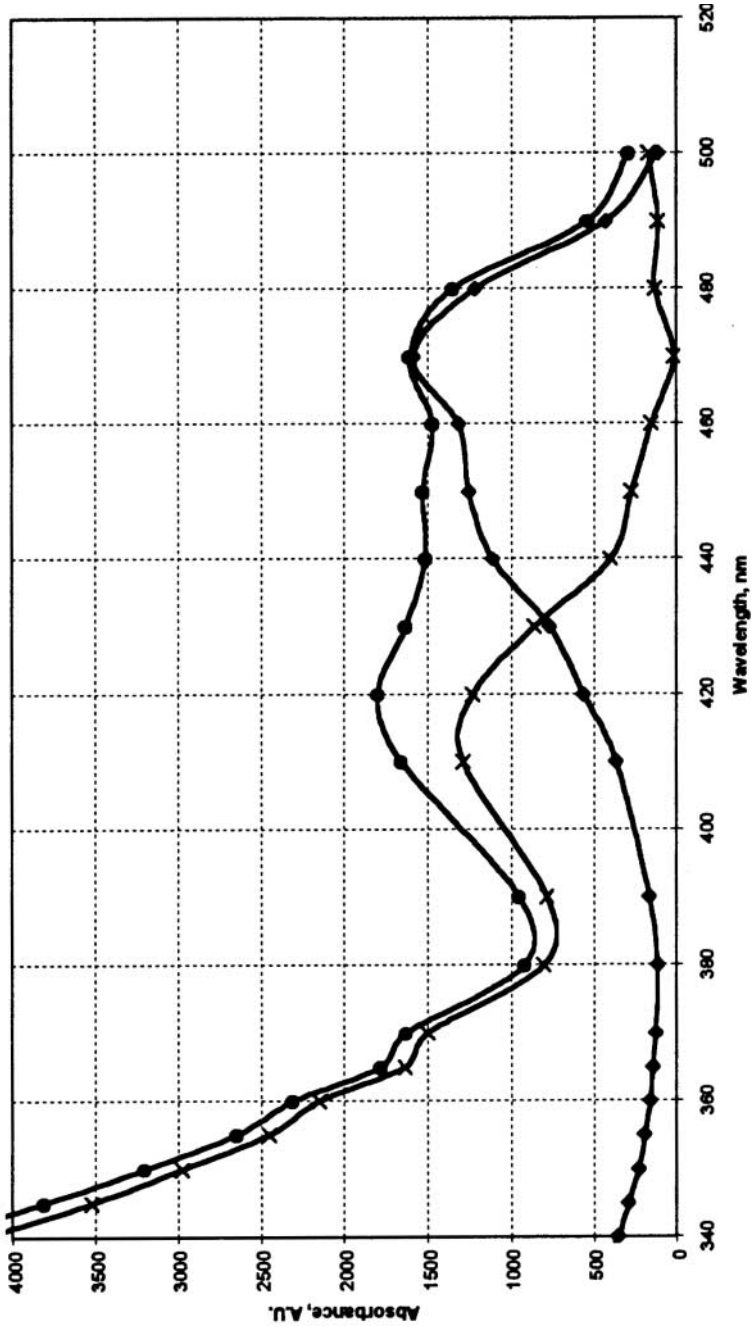

Figure 3. Deconvoluted spectrum of 1,2,4-tri-methoxylbenzene OH-radical products with the contribution from radical cations removed (×), the initial spectrum (●), and the scaled initial aromatic radical cation spectrum (◆).

used to predict the one-electron oxidation potentials for substituted benzenes for which experimental data are not available. One-electron oxidation potential data were obtained from the literature or by the mentioned procedure. These potentials and the measured reaction rate constants from Table 3 are summarized in Table 5 and plotted vs. each other in Fig. 4. Kinetic data from other authors have also been included. The reported $\log_{10} k$ of toluene and benzene should be taken with caution, and as maximum values, due to experimental difficulties of measuring such low reaction rate constants.

Table 5. One electron reduction potentials and rate constants of reaction with $CO_3^{\bullet -}$ of different substituted benzenes.

Substance	Rate constant ($M^{-1} s^{-1}$)	Ref.	E^0 V vs. NHE	Ref.
4-Nitrophenoxide ion	4.8×10^7	18	1.22	32
Chlorophenoxide ion	1.9×10^8	18	0.8	32
4-Cyanophenoxide ion	6.5×10^7	16	1.12	32
4-Bromoaniline	3.8×10^8	9	1.04	35
4-Methylaniline	9.1×10^8	9	0.92	35
Phenoxide ion	2.7×10^8	16	0.79	32
2,4,6-tri-Methyl phenolate	2.7×10^9	Table 3	0.49	36
4-Methoxyphenolate	1.3×10^9	16	0.54	32
4-Methylphenolate	1.1×10^9	Table 3	0.68	32
4-Methylphenol	1.5×10^8	Table 3		39[a]
Creosol	1.5×10^9	Table 3	0.54	36
4-Chloroaniline	4.3×10^8	9	1.01	35
2,6-di-Methoxyphenolate anion	1.4×10^9	Table 3	0.47	36
Syringic acid	1.3×10^9	Table 3	0.54	36
Veratric acid	7.3×10^6	Table 3	1.44	37 and 40[b]
3,5-di-Methoxyphenolate anion	5.9×10^8	Table 3	0.82	38 and 40[c]
Vanillate ion	1.1×10^9	Table 3	0.86	38 and 40[c]
Toluene	4.3×10^4	41	1.98	31 and 42
Benzene	3×10^3	41	2.2	31, 42, and 43
Tyrosine dianion	2.9×10^8	44	0.89	32
Methoxybenzene (anisole)	2.8×10^5	45	1.62	31

[a]Potential calculated using a pK_A of 10.3.
[b]Calculated using relationship in Ref.[37] and constants in Ref.[40]
[c]Calculated using relationship in Ref.[38] and constants in Refs.[24,40]

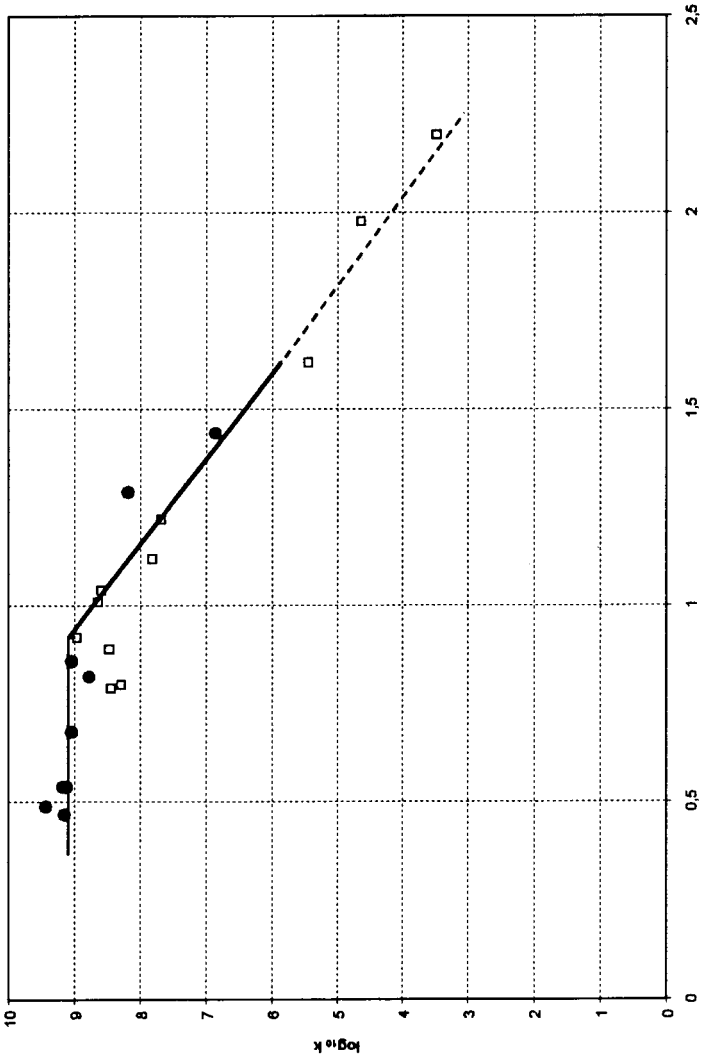

Figure 4. The logarithm of the rate constants of the reaction of $CO_3^{\bullet-}$ with different substituted aromatics vs. their oxidation potentials (E_0 vs. NHE). Values determined in this article (●) and reference data (□).

As can be seen in Fig. 4, there is a correlation between the oxidation potential of a substituted benzene and $\log_{10} k$. Oxidation potentials below approximately 0.9 V vs. NHE lead to diffusion controlled reaction rates, whereas those potentials above 0.9 V vs. NHE show a LFER.

If the reaction of the carbonate radical anion with aromatics proceeds through outer-sphere electron transfer, $\log k$ should be accurately described by the Marcus-equation[46]:

$$\ln k = \ln(\kappa Z) - \frac{\lambda_{12}}{4RT}\left(1 + \frac{\Delta G^0}{\lambda_{12}}\right)^2 \qquad \lambda_{12} = \frac{\lambda_{11} + \lambda_{22}}{2} \tag{10}$$

where κ is the transmission coefficient, Z the collision frequency, ΔG° the free energy of reaction, k the reaction rate and λ_{11} and λ_{22} the reorganization energies of each redox couple.

A least-squares fit of Eq. (10) to the data presented in Table 5, did not yield a good correlation. Especially in the case of the less reactive species, there are large deviations from the calculated theoretical line. This indicates that the reaction of the carbonate radical anion with aromatics does not proceed via a pure outer-sphere electron transfer process. As there are no steric or spin restrictions on the electron transfer from an aromatic to $CO_3^{\bullet-}$, the reaction may be an inner-sphere process involving orbital overlap in a transition state.

Using the plot in Fig. 4 and the mentioned relationship relating the oxidation potential of substituted aromatics to their substitution pattern,[37,38] we were able to assess the kinetics of the reaction of the carbonate radical anion with most lignin structures.

In Table 5 and Fig. 4 it can be seen that the phenol/phenolate forms of substituted phenols have different oxidation potentials. Therefore, their rate of reaction should vary with pH in accordance with the equations:

$$HA \overset{K_A}{\rightleftharpoons} H^+ + A^- \tag{11}$$

$$CO_3^{\bullet-} + HA \xrightarrow{k_{HA}} \text{prod} \tag{12}$$

$$CO_3^{\bullet-} + A^- \xrightarrow{k_{A^-}} \text{prod} \tag{13}$$

$$\frac{d[CO_3^{\bullet-}]}{dt} = -[CO_3^{\bullet-}](k_{HA}[HA] + k_{A^-}[A^-]) \tag{14}$$

$$[HA]_{tot} = [HA] + A^- \gg CO_3^{\bullet-} \tag{15}$$

$$k_{obs} = \frac{k_{HA} + k_{A^-}10^{pH-pK_A}}{1 + 10^{pH-pK_A}} \tag{16}$$

The behavior of cresol, using a reported pK_A-value of 10.3,[39] was calculated using Eq. (16), as shown in Fig. 5. As can be seen, the calculated curve closely follows the experimental data. Thus, it is possible to evaluate the kinetics of the reactions of the pure phenol/phenolate forms using the measured values over an experimentally accessible pH-interval if the pK_A-values are known. This is exemplified for vanillin (Fig. 5) where measurements were only possible on the vanillate form. For those structures with non-phenolic structures, e.g., *o*-methoxyphenoxyacetic acid, we see no pH-dependence.

2. Carbohydrates

Carbohydrates react with the carbonate radical anion with reaction rate constants in the range of 10^5–10^7 $M^{-1}s^{-1}$, Fig. 6 and Table 4. Interestingly, the reaction rate increases with increasing pH.

Since the carbonate radical is a mono-anion at all pH-values, the observed increase in reactivity must be attributed to the carbohydrates themselves. Assuming that this activation of the carbohydrates towards $CO_3^{\bullet-}$ depends on deprotonation, it is possible using Eqs. (11)–(16) together with the measured rate constants in Table 4 and a reported pK_A-value of 12.4 for glucose,[39] to calculate the rate constants for its neutral and deprotonated forms, as shown in Fig. 6. Cellobiose, having a similar structure and pK_A, shows the same relationship between reactivity and pH as that observed for glucose. This shows that the pH-dependence of these carbohydrates is associated with the reducing end-groups.

Surprisingly, in the case of methyl-β-D-glucopyranoside, with no reducing end-group, activation due to deprotonation was also observed, albeit only at a pH above 11. Using the measured rate constants, applying Eqs. (11)–(16), and assuming that the fully deprotonated form of methyl-β-D-glucopyranoside reacts as rapidly as fully deprotonated glucose, we can determine the pK_A-value of methyl-β-D-glucopyranoside to be approximately 14.4. To our knowledge, this is the first determination of the pK_A-value of a cellulose model compound.

It is reasonable to assume that the $CO_3^{\bullet-}$ reacts with anions by electron transfer. This should also be true for deprotonated carbohydrates. Experiments run at different temperatures revealed low activation energies with no significant pH-dependence. This result indicates that the reaction mechanisms at high and low pH are similar.

In a previous study on the reaction of $CO_3^{\bullet-}$ with alcohols,[11] Clifton and Huie suggested that the reactions are not pure hydrogen abstractions, but involve an additional interaction of the radical with the OH-linkage.

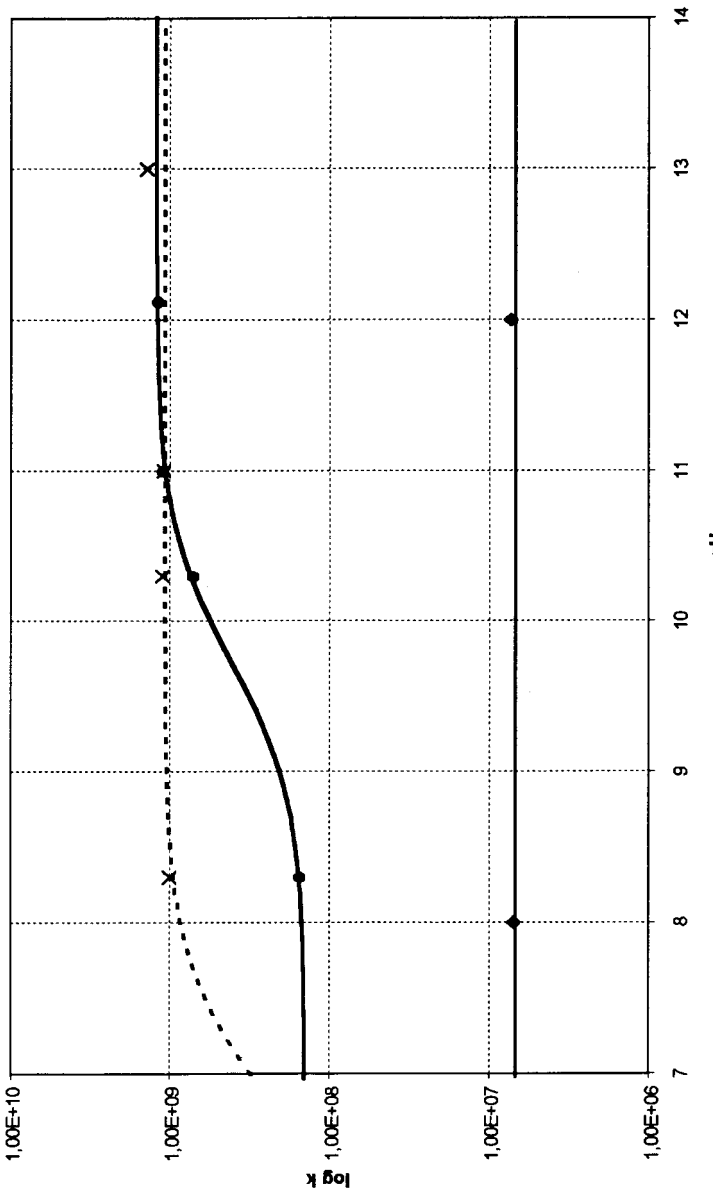

Figure 5. The logarithm of the rate constants for the reaction of $CO_3^{\bullet-}$ with three substituted benzenes as a function of pH; cresol (●), vanillin (×) and *o*-methoxyphenoxyacetic acid (◆). The lines were calculated using measured values and Eqs. (11)–(16).

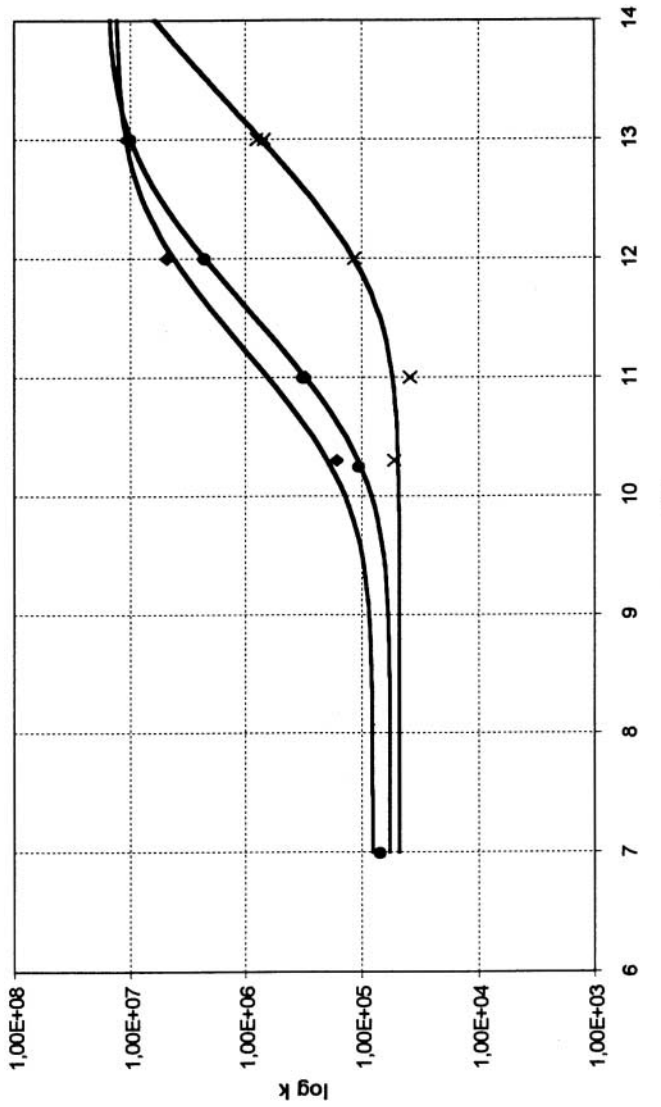

Figure 6. The logarithm of the rate constants for the reaction of $CO_3^{\bullet-}$ with glucose (●), cellobiose (◆) and methyl-β-D-glucopyranoside (×) as a function of pH. The calculated lines were calculated using measured values from Table 4 and Eqs. (11)–(16).

This indicates that these reactions proceed via an electron/proton transfer mechanism. Neutral carbohydrates may react in a similar way.

3. The Carbonate Radical in Pulp

The kinetic data obtained show that the carbonate radical has a higher reactivity towards lignin-like structures than towards carbohydrates. This kinetic selectivity should also manifest itself in pulp. More selective delignification should result because of carbonate ion scavenging of OH-radicals to give $CO_3^{\bullet-}$. Indeed, an increased selectivity is observed in bleaching experiments when carbonate is used as base.[21] Since the carbonate radical has a longer lifetime than the hydroxyl radical, $CO_3^{\bullet-}$ is able to diffuse short distances through the fibre and, thus, enable the kinetic selectivity to manifest itself. The reactivity of $CO_3^{\bullet-}$ towards different lignin constituents and carbohydrates is shown in Fig. 7.

The increased reactivity observed, as well as the pK_A-value obtained for methyl-β-D-glucopyranoside, indicates that glucose units in the cellulose polymer should be activated towards oxidative reactions by deprotonation as the pH is raised. The extent of such activation will depend on the oxidant and may be of importance in technical processes running at high pH, i.e., pulping and oxygen bleaching.

Regarding selectivity, it should be noted that the carbonate radical can attack carbohydrates and should therefore be beneficial only in systems which still contain some lignin structures. In such systems, the carbonate radical has a kinetic selectivity of approximately 10^3–10^4 depending on the pH and compounds involved.

From Fig. 7 it can be concluded that the maximum reactivity difference between carbohydrates and most phenolics lies at about pH 10.5. In pulp systems where the carbonate radical is formed, the maximum selectivity should thus be expected at about this pH. This is conveniently near the pH of a 1:1 HCO_3^-/CO_3^{2-}-buffer solution.

CONCLUSIONS

Carbonate radicals formed in a pulp system can oxidise both lignin structures and carbohydrates present, although they show a significant kinetic selectivity towards lignin. For most pulp bleaching, where carbonate can be found in solution, the carbonate will act as a scavenger of hydroxyl radicals and will produce $CO_3^{\bullet-}$. The latter can diffuse through

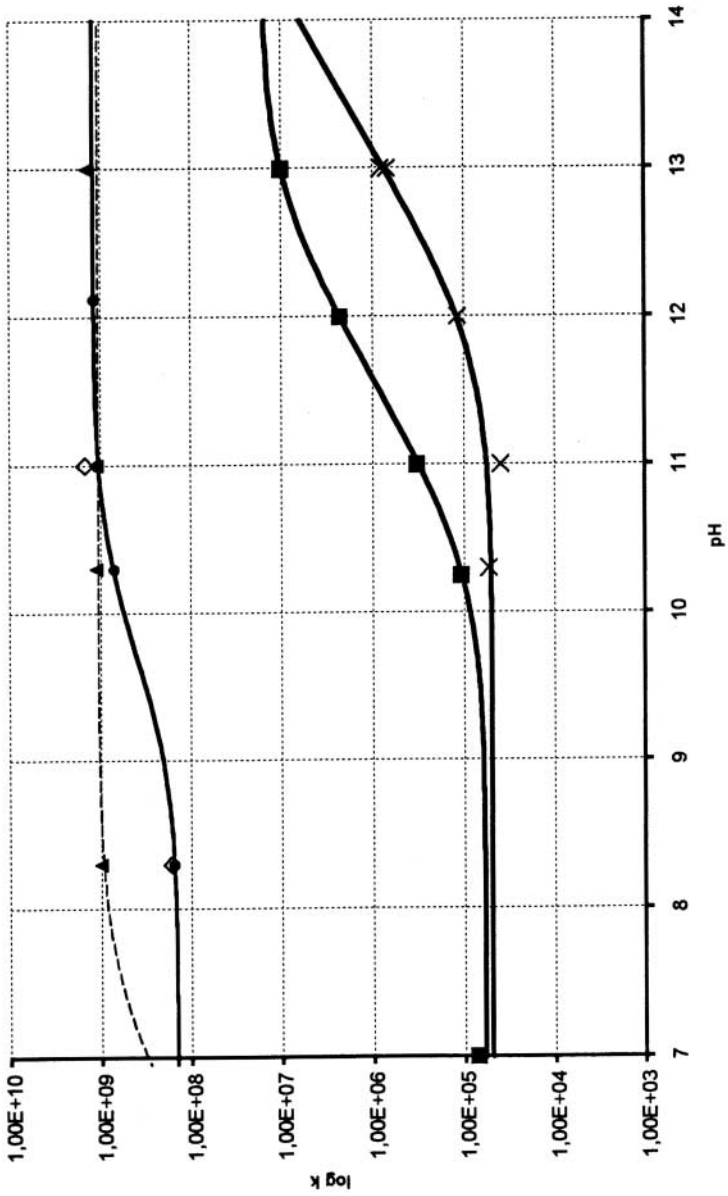

Figure 7. The logarithm of the rate constants for the reaction of $CO_3^{\bullet-}$ with different lignin and carbohydrate model compounds vs. pH. The lines were calculated using measured values from Tables 3 and 4 and Eqs. (11)–(16). Methyl-β-D-glucopyranoside (×), glucose(■), vanillin (▲), cresol (●) and creosol (◇).

the pulp and a kinetic selectivity for lignin reaction will manifest itself. For new processes utilising carbonate as base, such effects will be enhanced due to the high carbonate concentrations applied.

Kinetic studies using the carbonate radical have shown that carbohydrates are activated towards oxidation due to deprotonation as the pH is increased. Surprisingly, this was also the case for methyl-β-D-glucopyranoside, for which a pK_A-value of about 14.4 was estimated. Such an activation of this cellulose model compound, representing an intra-molecular glucose unit, implies that the cellulose itself will be activated towards oxidation at high pH. This could lead to a lowered selectivity for those technical processes which require a high pH.

Lignin structures containing aromatic rings react with the carbonate radical anion by electron transfer. In the case of carbohydrates, it seems that the radical reacts through a hydrogen abstraction and/or electron/proton transfer mechanism at low pH, while deprotonated carbohydrates react through electron transfer at high pH.

The relationships between kinetics and oxidation potentials obtained for aromatics can be used, together with previous knowledge, to calculate the reactivity of most lignin structures towards the carbonate radical. Using such thermodynamic knowledge for this and other radicals or oxidants, it might be possible to find the optimal oxidative properties for future "green" oxidants.

REFERENCES

1. Gierer, J.; Reitberger, T.; Yang, E.; Yoon, B.-H. Formation and involvement of radicals in oxygen delignification studied by the autoxidation of lignin and carbohydrate model compounds. J. Wood Chem. and Techn. **2001**, *4* (21), 313–341.
2. Huie, R.E.; Clifton, C.L.; Neta, P. Electron transfer reaction rates and equilibria of the carbonate and sulfate radical anions. Radiat. Phys. Chem. **1991**, *5* (38), 477–481.
3. Lilie, J.; Hanrahan, R.J.; Henglein, A. Oxygen(−1) transfer reactions of the carbonate radical anion. Radiat. Phys. Chem. **1978**, *5* (11), 225–227.
4. Chawla, O.P.; Fessenden, R.W. Electron spin resonance and pulse radiolysis studies of some reactions of peroxysulfate (SO4.1,2). J. Phys. Chem. **1975**, *24* (79), 2693–2700.
5. Bonini, M.G.; Radi, R.; Ferrer-Sueta, G.; Ferreira, A.M.D.C.; Augusto, O. Direct EPR detection of the carbonate radical anion produced from peroxynitrate and carbon dioxide. J. of Biol. Chem. **1999**, *274* (16), 10802–10806.

6. Eriksen, T.E.; Lind, J.; Merenyi, G. On the acid-base equilibrium of the carbonate radical. Radiat. Phys. Chem. **1985**, (26), 197.
7. Umschlag, T.; Herrmann, H. The carbonate radical (HCO3/CO3-) as a reactive intermediate in water chemistry. Kinetics and modelling. Acta Hydrochim. Hydrobiol. **1999**, *4* (27), 214–222.
8. Chen, S.N.; Hoffman, M.Z. Rate constants for the reaction of the carbonate radical with compounds of biochemical interest in neutral aqueous solution. Radiat. Res. **1973**, *1* (56), 40–47.
9. Elango, T.P.; Ramakrishnan, V.; Vancheesan, S.; Kuriacose, J.C. Reaction of the carbonate radical with substituted anilines. Indian Acad. Sci. Chem. Sci. **1984**, *1* (93), 47–52.
10. Kuz′min, V.A.; Chibisov, A.K. Photochemical oxidation of water by aromatic ketones, benzo- and napthoquinones. Teor. Eksp. Khim. **1971**, *3* (7), 403–407.
11. Clifton, C.L. Huie, R.E. Rate constants for some hydrogen abstraction reactions of the carbonate radical. Int. J. Chem. Kinet. **1993**, *3* (25), 199–203.
12. Chen, S.-N.; Cope, V.W.; Hoffman, M.Z. Behaviour of carbon trioxide (−) radicals generated in the flash photolysis of carbonato-amine complexes of cobalt(III) in aqueous solution. J. Phys. Chem. **1973**, *9* (77), 1111–1116.
13. Draganic, Z.D.; Negron-Mendoza, A.; Sehested, K.; Vujosevic, S.I.; Navarro-Gonzales, R.; Albarran-Sanchez, M.G.; Draganic, I.G. Radiolysis of aqueous solutions of ammonium bicarbonate over a large dose range. Radiat. Phys. Chem. **1991**, *3* (38), 317–321.
14. Baverstock, K.; Cundall, R.B.; Adams, G.E.; Redpath, J.L. Selective free radical reactions with proteins and enzymes: the inactivation of alpha-chymotrypsin. Int. J. Radiat. Biol. Relat. Stud. Phys., Chem. Med. **1974**, *1* (26), 37–46.
15. Saunders, B.B.; Gorse, R.A.J. Reactions of diethylhydroxylamine with radiolytically produced radicals in aqueous solutions. J. Phys. Chem. **1979**, *13* (83), 1696–1701.
16. Huie, R.E.; Shoute, L.C.T.; Neta, P. Temperature dependance of the rate constants for reactions of the carbonate radical with organic and inorganic reductants. Int. J. Chem. Kinet. **1991**, *23* (6), 541–552.
17. Faraggi, M.; Weinraub, D.; Broitman, F.; DeFelippis, M.R.; Klapper, M.H. One-electron oxidations of ferrocenes: a pulse radiolysis study. Radiat. Phys. Chem. **1988**, *32* (2), 293–297.
18. Moore, J.S.; Phillips, G.O.; Sosnowski, A. Reaction of the carbonate radical anion with substituted phenols. Int. J. Radiat. Biol. Relat. Stud. Phys., Chem. Med. **1977**, *6* (31), 603–605.

19. Pikaev, A.K.; Gogolev, A.V.; Shilov, V.P.; Fedoseev, A.M. Reactivity of ions of actinides towards free radicals in irradiated aqueous solutions. Isotopenpraxis **1990**, *10* (26), 465–469.
20. Czapski, G.; Lymar, S.V.; Schwarz, H.A. Acidity of the carbonate radical. J. Phys. Chem. **1999**, *A* (103), 3447–3450.
21. Patent, Pulp Delignification Process, PCT/SE00/00172.
22. Thompson, N.S.; Mih, J.-F. The effect of liquor composition on the rate of reaction of lignin model compound acetoguaiacone in oxygen and alkali. J. Wood Chem. and Tech. **1983**, *2* (3), 145–159.
23. Lymar, S.V.; Hurst, J.K. Rapid reaction between peroxynitrite ion and carbon dioxide: implications for biological activity. J. Am. Chem. Soc. **1995**, (117), 8867–8868.
24. Beckman, J.S.; Beckman, T.W.; Chen, J.; Marshall, P.A.; Freeman, B.A. Apparent hydroxyl radical production by peroxynitrite: implications for edothelial injury from nitric oxide and superoxide. Proc. Natl. Acad. Sci. USA. **1990**, (87), 1620–1625.
25. Beckman, J.S. Oxidative damage and tyrosine nitration from peroxynitrite. Chem. Res. toxicol. **1996**, (9), 836–844.
26. Lymar, S.V.; Hurst, J.K. Carbon dioxide: physiological catalyst for peroxynitrite-mediated cellular damage or cellular protectant? Chem. Res. Toxicol. **1996**, *5* (9), 845–850.
27. Baxendale, J.H.; Busi, F. *The Study of Fast and Transient Species by Electron Pulse Radiolysis*, 1st Ed. NATO Advanced Study Institutes Series, Reidel Publishing Company: Dordrech, 1982, Vol. D.
28. Buxton, G.V.; Greenstock, C.L.; Helman, W.P.; Ross, A.B. Critical review of rate constants for reactions of hydrated electrons, hydrogen atoms and hydroxyl radicals in aqueous solution. J. of Phys. and Chem. Ref. Data. **1988**, *2* (17), 513–886.
29. Ek, M.; Gierer, J.; Jansbo, K.; Reitberger, T. Study on the selectivity of bleaching with oxygen-containing species. Holzforschung **1989**, *6* (43), 391–396.
30. Eriksen, T.E.; Lind, J.; Reitberger, T. A computerized pulse radiolysis system. Chem. Scr. **1976**, (10), 5–7.
31. Jonsson, M.; Lind, J.; Reitberger, T.; Eriksen, T.E.; Merenyi, G. Redox chemistry of substituted benzenes. The one-electron potentials of methoxy-substituted benzene Radical Cations. J. Phys. Chem. **1993**, *97* (43), 11278–11282.
32. Lind, J.; Shen, X.; Eriksen, T.E.; Merenyi, G. The one-electron reduction potential of 4-substituted phenoxyl radicals in water. J. Phys. Chem. **1990**, *2* (112), 479–482.

33. Baciocchi, E.; Bietti, M.; Lanzalunga, O. Mechanistic aspects of beta-bond-cleavage of aromatic radical cations. Acc. Chem. Res. **2000**, (33), 243–251.
34. Sehested, K.; Holcman, J. Anisole radical cation reactions in aqueous solution. J. Phys. Chem. **1976**, *14* (80), 1642–1644.
35. Jonsson, M.; Lind, J.; Eriksen, T.E.; Merenyi, G. Redox and acidity properties of 4-substituted aniline radical cations in water. J. Am. Chem. Soc. **1994**, *116* (4), 1423–1427.
36. Jonsson, M.; Lind, J.; Reitberger, T.; Eriksen, T.E.; Merenyi, G. Free radical combination reactions involving phenoxyl radicals. J. Phys. Chem. **1993**, *31* (97), 8229–8233.
37. Jonsson, M.; Lind, J.; Merenyi, G.; Eriksen, T.E. N–H bond dissociation energies, reduction potentials and pKas of multi-substituted anilines and aniline radical cations. J. Chem. Soc. Perkin. Trans. **1995**, (2), 61–65.
38. Jonsson, M.; Lind, J.; Eriksen, T.E.; Merenyi, G. Oxygen–hydrogen bond strengths and one-electron reduction potentials of multi-substituted phenols and phenoxy radicals. Predictions using free energy relationships. J. Chem. Soc. Perkin. Trans. **1993**, (2), 1567–1568.
39. Serjeant, E.P.; Dempsey, B. *Ionisation Constants of Organic Acids in Aqueous Solutions*, 1st Ed.; IUPAC Chemical Data Series - No. 23, Pergamon Press: Oxford, 1979.
40. Hansch, C.; Leo, A.; Taft, R.W. A survey of hammett substituent constants and resonance and field parameters. Chem. Rev. **1991**, *2* (91), 165–195.
41. Chen, S.-N.; Hoffman, M.Z.; Parsons, G.H. Reactivity of the carbonate radical toward aromatic compounds in aqueous solution. J. Phys. Chem. **1975**, *18* (79), 1911–1912.
42. Pearson, R.G. Ionization potentials and electron affinities in aqueous solution. J. Am. Chem. Soc. **1986**, *20* (108), 6109–6114.
43. Nicholas, A.M.P.; Arnold, D.R. Thermochemical parameters for organic radicals and radical ions. Part 1. The estimation of the pKa of radical cations based on thermochemical calculations. Can. J. Chem. **1982**, *17* (60), 2165–2179.
44. Adams, G.E.; Aldrich, J.E.; Bisby, R.H.; Cundall, R.B.; Redpath, J.L.; Willson, R.L. Selective free radical Reactions with proteins and enzymes. Reactions of inorganic radical anions with amino acids. Radiat. Res. **1972**, *49* (2), 278–289.
45. Radiation Chemistry Data Centre, Notre Dame Radiation Laboratory.
46. Marcus, R.A. The theory of oxidation–reduction reactions involving electron transfer. III. Applications to data on the rates of inorganic redox reactions. J. Chem. Phys. **1957**, (26), 872–877.

MARCEL DEKKER, INC. • 270 MADISON AVENUE • NEW YORK, NY 10016